Journal of Mechatronics, Electrical Power, and Vehicular Technology 17 (2026) 168-179

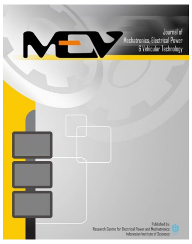

Journal of Mechatronics, Electrical Power, and Vehicular Technology

CrossMark

e-ISSN: 2088-6985
p-ISSN: 2087-3379

mev.brin.go.id

Design of a low harmonic five-level inverter based on a wind power plant using a DC generator with LCL filter

Setiyono*, Bambang Dwinanto, Dyah Nur'ainingsih

Department of Electrical Engineering, Gunadarma University
Jl. Margonda Raya 100 Pondokcina, Depok, Indonesia

Abstract

Wind energy is one of the green energy sources that can decrease reliance on fossil fuels such as oil and coal. Wind turbines harness the kinetic energy of the wind and transform it into mechanical energy, which is subsequently converted into electrical energy using a DC generator. The generated DC voltage is transformed into AC voltage by an inverter unit. However, conventional inverters generally produce square-wave outputs with high total harmonic distortion (THD), whereas AC power systems ideally require sinusoidal waveforms with low harmonic content. This research proposes the design of a renewable energy–based power supply system capable of generating both DC and AC voltages for low-power applications. The novelty of the proposed system lies in the use of a five-level inverter with fewer switching devices than the cascaded inverter topology, combined with a T-model inductive-capasitive-inductive (LCL) filter to suppress harmonic distortion at the inverter output. The method involves modeling and simulating the system design using MATLAB Simulink. Simulation results show that the five-level inverter produces an output voltage amplitude of 270 V at 50 Hz with a THD of 28.48 %. After applying the LCL filter (L1 = L2 = 0.01 H and C = 1 mF), the THD decreases to 2.56 % for a 10 Ω resistive load, 2.61 % for an RL load (100 Ω, 0.8 mH), and 2.54 % for an RC load (10 Ω, 1 μF). These values comply with the IEEE 519 standard requiring THD below 5 %. Therefore, the proposed system has potential for small-scale renewable energy applications.

Keywords: DC generator; five-level inverter; LCL filter; renewable energy; total harmonic distortion; wind energy; wind power plant.

I. Introduction

Indonesia currently relies heavily on PLN (State Electricity Company) and fossil fuels (coal and oil) to meet its electricity needs. To reduce this dependence, the government is shifting its focus to abundant wind energy. The target is for renewable energy capacity to reach 52–62 GW by 2030, requiring an additional 6 GW of new projects annually [1].

Wind energy is estimated to meet up to 33 % of the Earth's energy needs in the future [2]. Renewable energy technologies produce significantly lower lifecycle carbon emissions than fossil fuels; therefore, their development and use, such as wind turbines, help reduce overall emissions and support the clean energy transition [3]. Indonesia has a high wind energy potential, especially in the southern part of the equator, including Nusa Tenggara Timur (NTT), Nusa Tenggara Barat (NTB), and South Sulawesi [4][5]. Electrical energy generated from wind power is stored in batteries, while AC voltage can be obtained by converting DC voltage using an inverter circuit.

* Corresponding Author. setiyono@staff.gunadarma.ac.id (Setiyono)

https://doi.org/10.55981/j.mev.2026.1138

Received 29 September 2025; 1st revision 24 February 2026; 2nd revision 16 June 2026; accepted 9 July 2026; available online 30 July 2026; published 31 July 2026

How to Cite: Setiyono *et al.*, "Design of a low harmonic five-level inverter based on a wind power plant using a DC generator with LCL filter," *Journal of Mechatronics, Electrical Power, and Vehicular Technology*, vol. 17, no. 1, pp. 168-179, July, 2026.

However, simple inverters typically produce square waveforms with high Total Harmonic Distortion (THD), which can cause overheating, power losses, and potential damage to electrical and electronic equipment [6].

Some efforts to reduce these harmonics use active passive filters [7]. Another effort to achieve lower harmonic distortion is by changing the inverter output voltage square wave into a wave that resembles a sinusoidal waveform [8]. The method is to generate a multilevel staircase output voltage waveform [9]. This multilevel inverter technology can be applied to renewable energy sources with Variable Frequency Drives (VFD), Alternating Current Control, Flexible AC Transmission Systems [10], vehicle electricity, and can also be applied to lighting systems for fish farming in ponds [11]. This study aims to model a battery charging system supplied by a DC generator driven by wind energy and integrated with a five-level multilevel inverter for AC power generation. The proposed system is capable of producing both DC and AC voltages of 14.65 V and 260 V, respectively, while operating at low frequencies of 50 Hz and 200 Hz through the control of a five-level inverter using five switching devices. This study proposes the development of a wind energy–based five-level inverter topology with fewer switching devices and the implementation of an LCL filter to reduce the Total Harmonic Distortion (THD) to below 5 % using MATLAB Simulink tools.

II. Materials and Methods

The proposed system is composed of a wind power generation unit, a DC generator, a five-level inverter, and an LCL output filter, as shown in Figure 1. The wind turbine captures the kinetic energy of the wind and converts it into mechanical energy, which is then transformed into electrical energy by a DC generator. The generated DC voltage is then supplied to the five-level inverter to produce an AC output voltage that still contains relatively significant harmonic components. An LCL filter is installed at the inverter's output to attenuate high-frequency switching harmonics process. The filtered output voltage is then fed into a transformer to achieve the voltage level required by the AC load. The transformer is selected to increase the inverter AC output voltage due to its high efficiency, low power losses, and the absence of additional harmonic generation. In addition to providing galvanic isolation, which enhances system safety and reliability, the transformer has a simple structure that does not require additional control systems, making it more economical and easier to integrate into conventional power systems. Therefore, the use of a transformer is considered more appropriate than power electronic-based solutions for increasing the AC voltage in inverter-based wind power generation systems. To assess the robustness and performance of the proposed inverter, the system is evaluated under three load conditions: resistive (R), resistive–inductive (RL), and resistive–capacitive (RC) loads. Figure 2 presents the overall system design modeling implemented using MATLAB/Simulink.

A. Workflow methodology

Figure 1 shows the overall research methodology employed in this study. Initially, the wind turbine harnesses the kinetic energy available in the wind and converts it into mechanical energy through the rotational motion of the turbine blades. This energy is subsequently transferred to a DC machine; the generated DC voltage is then utilized as the DC-link voltage source of the inverter system. The DC power is converted into AC power using a five-level inverter topology driven by a sinusoidal pulse width modulation (SPWM) control strategy.

This inverter topology generates a multilevel stepped AC waveform, which reduces harmonic

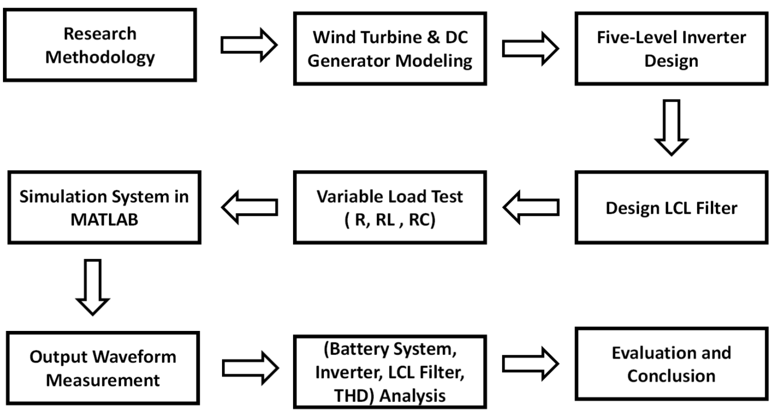

Figure 1. Research flow.

distortion compared to conventional two-level inverters. However, the inverter output voltage still contains high-frequency harmonics caused by the switching process of semiconductor devices. To mitigate these unwanted harmonics and improve the quality of the output waveform, the inverter output voltage is passed through an LCL filter. This filter effectively reduces the high-frequency switching harmonics produced by the inverter, thereby smoothing the stepped voltage waveform and generating an output waveform that closely approximates a sinusoidal waveform. Furthermore, in order to obtain an AC voltage level that is suitable for practical load requirements or for integration into distribution systems, the filtered AC voltage is increased using an AC transformer.

The proposed system performance is assessed under various loads to represent realistic operating scenarios commonly encountered in power electronic-based energy systems. These load variations allow the investigation of system behavior under different electrical characteristics. The performance evaluation is carried out through harmonic analysis based on Fast Fourier Transform (FFT), with particular focus on calculating the THD of the output voltage as a key indicator of power quality.

The entire system configuration is modeled and simulated using MATLAB/Simulink, which enables comprehensive analysis of the system operation and performance. Through the simulation results, it is expected that the combination of a five-level inverter, LCL filter, and transformer will be able to produce output voltages with low THD values across different load conditions. This outcome would demonstrate that the proposed system design is capable of delivering good power quality and is therefore suitable for potential implementation in wind power generation applications.

Meanwhile, Figure 2 presents the detailed electrical system design of the five-level inverter supplied by a DC generator and integrated with an LCL filter. Figure 3 is a design system modelling using the MATLAB Simulink tool. Table 1 presents the element parameter values used in system design.

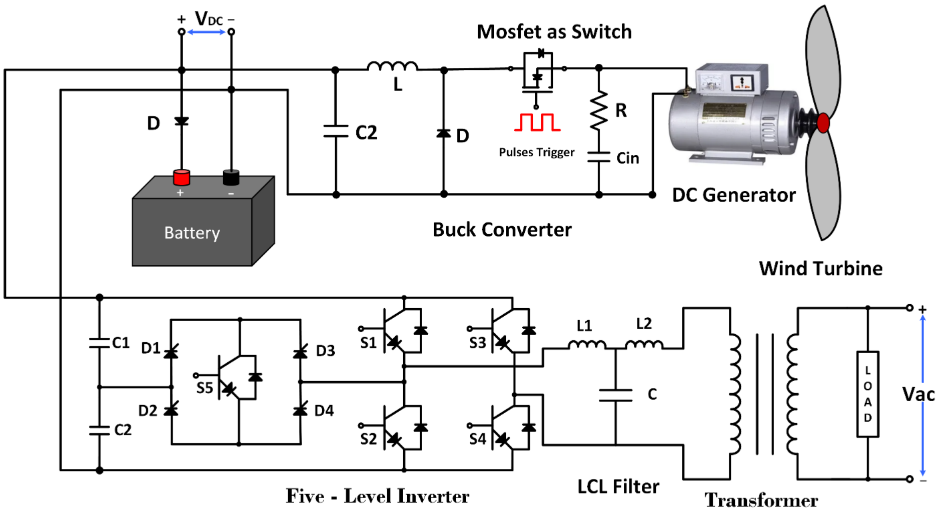

Figure 2. System design.

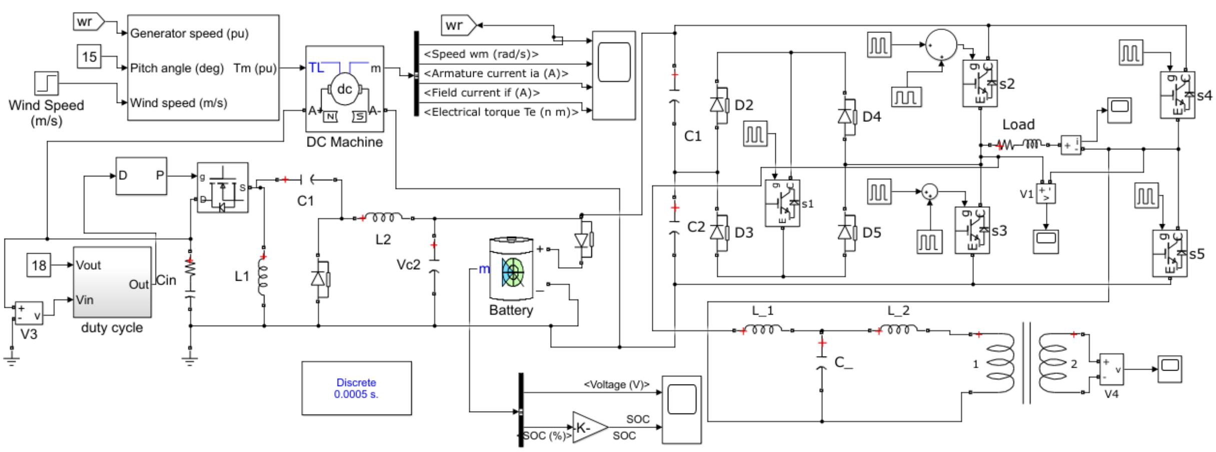

Figure 3. Design system modeling.

Table 1.
The technical parameters of the components used in the system design.

Parameter Name	Spesification
Wind turbine	Nominal power output 700W, electrical generator power 300 VA, wind speed 2 m/s, power base 1 pu base rot. speed 1.2 pu, pitch angle beta = 0
DC generator (permanent magnet)	Ra=0.6 ohm, La = 0.012 ohm, torque 100 Nm/A, initial speed 1.2 pu, total inertia 1
Buck converter	C1=C2=200 mF, L=0.0133 H, diode, mosfet, switching frequency (Fs) 3 kHz
Battery	Lead acid, 12 V, rated current capacity 180 Ah
Five-level inverter	Inverter S1- S5 = transistors, Fs S1- S4 50 Hz (duty cycle 50 %) fullwave bridge (diodes D1, D2, D3, D4) Fs S5 = 200 Hz (duty cycle 50 %)
Transformer	R1 = 0,000557 ohm, L1 = 0.000073 H, R2 = 0.193 ohm, L2 = 0.02465 H, V1 = 12 V, V2 = 220 V
Filter LCL	L1 = L2=0.01 H, C = 1mF
Load	Resistive (R = 10 ohm), resistive inductive (R = 10 ohm, 0.8 mH), resistive capasitive (R= 10 ohm, C = 1 uF)

B. Wind turbine aerodynamics

The moving wind can be converted into kinetic energy through a wind turbine, which is needed as a prime mover for the generator. Wind turbines are generally classified into two main types: horizontal axis wind turbines and vertical axis wind turbines [12]. Wind power is currently dominated by horizontal axis wind turbines [13].

This power can then be expressed as mechanical power and notated by equation (1) [14][15]:

$$P_m = \frac{1}{2} C_p(\lambda, \beta)\rho A v^3 \quad (1)$$

where P_m is the mechanical power (W), C_p is the coefficient of power, λ is the tip speed ratio , ρ is the air mass density, A is the rotor disk area, β is blade pitch angle, and v is the wind speed. The rotor area is determined using the following equation $P_m = T\omega$, where T is the torque of the rotor (Nm) [16].

C. DC generator

This DC machine is the only machine that is easy to regulate the rotational speed. With the development of power electronics, speed control is easier and cheaper. In this machine, if a coil located between the magnetic poles is rotated with a constant rotational speed (ω), then at both ends of the coil will arise an electrical motive force (EMF) [17]. Figure 4 is the DC Generator equivalent circuit.

Figure 4 illustrates the electrical circuit of a DC machine. The magnitude of the induced EMF generated by the armature coil depends on the magnitude of the flux [18] produced by the magnetic poles, which are reinforced with field coils of varying value, the engine speed (N), and the number of conductors throughout the armature slot, and is expressed in equation (2) [19]:

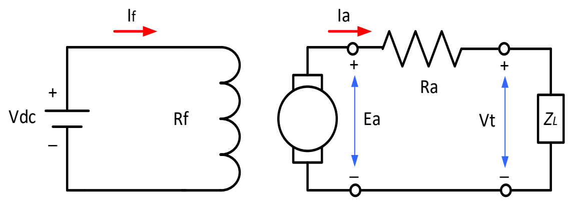

Figure 4. Equivalent circuit DC generator.

$$E_a = \frac{\phi.P.n.Z}{a} \quad (2)$$

Equation (2) can be rearranged as:

$$E_a = \frac{\phi.P.N.Z}{a.60} x \frac{2\pi}{2\pi}$$
$$= \frac{1}{2\pi}.2\pi n.\phi.Z.\frac{P}{a}$$

where E_a is armature EMF (volt), ϕ is flux per pole (wb), N is engine rotational speed (rpm), n is engine revolutions per second (rps), P is number of poles, and a is number of armature coils in parallel connection, Z is total number of armature conductors, π is constant (3.14). The commutator is a key component of a DC generator that converts armature current into direct current supplied to the load. The torque generated by the armature (T_a) can be expressed by equation (3):

$$T_a = 0.117.\frac{E_a I_a}{n} \quad (3)$$

where I_a is armature current.

D. Battery and charger controller

Battery energy storage systems have a vital role in power systems integrated with renewable energy by reducing generation intermittency and enhancing voltage and frequency stability [20]. Various batteries used for energy storage include lead-acid and lithium-ion types. Battery selection depends on several factors such as capacity, output voltage, depth of discharge (DoD), and state of charge (SoC) [21]. SoC represents the ratio of the stored energy to the battery's maximum capacity (0–100 %), while DoD is the inverse of SoC. For example, a fully charged battery has SoC = 100 %

and DoD = 0 %. The SoC value can be expressed in equation (4) [22]

$$SOC_t = SOC_{t-1} + \Delta SOC \quad (4)$$

where SOC_t, SOC_{t-1}, ΔSOC are variations in State of Charge, t is current time and Δ is change of SoC.

E. Controllers and buck converter

The DC generator produces 132 V, while battery charging requires about 12 V; thus, a voltage step-down circuit is needed. Commonly used DC–DC converters include boost, buck, and buck–boost converters. The first type of converter increases the input voltage, the second type reduces the input voltage to a lower level [23], while in the third type, the output voltage can be stepped up or stepped down by controlling the duty cycle of the switching signal and polarity configuration [24]. The applications of these three types of converters are widespread, covering industrial systems, residential applications, and various other electronic devices [25]. In this research, the chosen type of DC-DC converter is the asynchronous buck converter type, as shown in Figure 5. The operation can be divided into two modes, namely operating mode 1 when the MOSFET switch is turned ON and operating mode 2 when the MOSFET switch is turned OFF.

F. LCL filter

Compared to L-type or LC-type filters, the LCL (T-model) filter provides stronger harmonic attenuation with a steeper attenuation slope, resulting in a more sinusoidal output waveform and compliance with power quality standards such as IEEE 519. Figure 6 shows an LCL filter that consists of two inductors, one placed on the inverter side and the other on the load or grid side, and a capacitor connected between these two inductors. This configuration causes the filter to operate as a third-order low-pass filter, which is effective in suppressing high-frequency switching components [26].

The selection of LCL filter component values is generally related to the filter resonance frequency, which is designed to be well below the switching frequency, can be expressed by equation [27].

$$L_1 = \frac{V_{dc}}{6.f_{sw}.\Delta I_{pp}} \quad (5)$$

$$L_2 = c.L_1$$

where V_{dc} is dc link voltage (V), f_{sw} = switching frequency (Hz), ΔI_{pp} is maximum current, C is a constant. After L_1 and L_2 are selected, the capacitor value C is calculated using equation (6):

$$C = \frac{L_1 + L_2}{(2\pi f_{sw})^2 L_1.L_2} \quad (6)$$

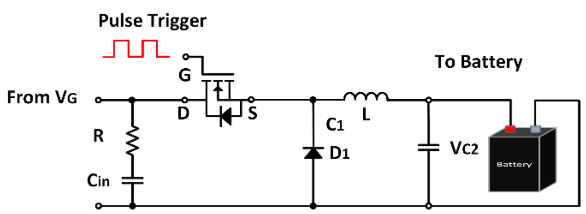

Figure 5. Buck converter with battery load.

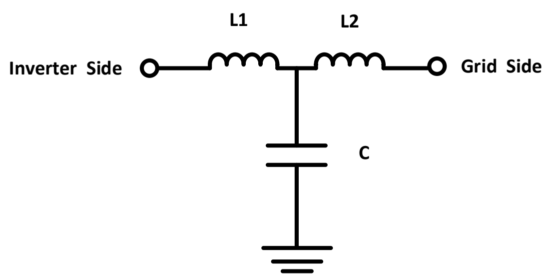

Figure 6. LCL filter design.

III. Results and Discussions

A. Battery charging analysis

The battery charging subsystem uses a buck converter to regulate the variable DC voltage. The converter consists of a PWM-controlled MOSFET, inductor (L), diode (D), and capacitor (C2), with the output voltage controlled by the PWM duty cycle. When the MOSFET is ON, energy is transferred from the generator to the inductor and battery, while when it is OFF, the stored energy flows through the diode to maintain continuous current. The capacitor reduces voltage ripple and improves charging stability, while the diode prevents reverse current, ensuring stable battery charging and a reliable DC supply for the inverter stage.

B. Five-level inverter analysis

The demand for low-harmonic distortion inverters continues to increase [28]. Multilevel inverters, formed by cascading several inverter stages, are designed to produce output voltages with reduced waveform distortion. Common topologies include diode-clamped, flying capacitor, and cascaded H-bridge converters [29]. However, those configurations typically require many switches and isolated DC sources, increasing system complexity and cost [30]. To address this issue, this study proposes a five-level inverter using only five switches, reducing three switches compared to the conventional cascaded H-bridge topology. This configuration offers a simpler structure, higher efficiency, and lower switching power requirements [31], while minimizing power losses by lowering the number of power switches [32] and modifies the inverter topology to improve the output waveform [33]. As seen in Figure 2, the inverter is composed of an H-bridge (S1–S4) with an additional switch S5 to generate output voltage levels, and diodes D1–D4 acting as a bridge rectifier supplying the load. Switches S2 and S4 generate the zero level, S1 and S4 produce the positive Vdc level, S2 and S3 generate the negative –Vdc level, while S4–S5 and S3–S5 form the Vdc/2 and –Vdc/2 levels, respectively.

1) Operation Mode Level 0

Figure 7 illustrates that a zero-voltage output level is achieved when switches S2 and S4 are activated. Under this switching condition, the load terminals are short-circuited, resulting in a zero voltage across the load.

2) *Operation Mode Level Vdc/2*

In Figure 8 voltage level Vdc/2 is generated by turning on switches S4 and S5. Only in this condition is the bottom source connected to the load, producing a voltage of Vdc/2 across the load.

3) *Operation Mode Level Vdc*

Figure 9 explains that by turning on switches S1 and S4, the Vdc voltage level can be obtained. During this switching operation, both voltage sources are connected to the load, resulting in an increased output voltage level.

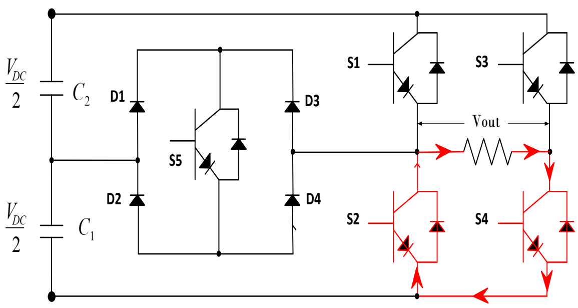

Figure 7. The current flow at level 0.

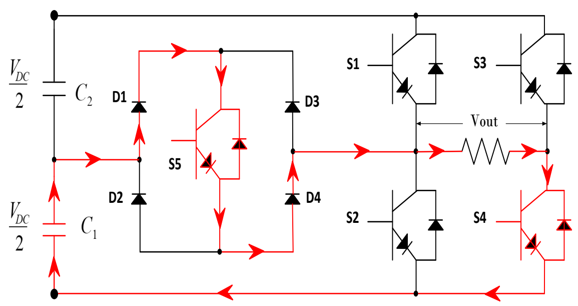

Figure 8. The direction of the current flow at the Vdc/2 level.

4) *Operation Mode Level –Vdc*

Figure 10 explains the direction of power flow in the –Vdc level mode. The –Vdc voltage level can be obtained by operating switches S2 and S3. Both source voltages are connected to the load with negative polarity.

5) *Operation Mode Level –Vdc/2*

Figure 11 shows that the –Vdc/2 voltage level is obtained by closing switches S3 and S5. In this operating condition, the upper DC source is connected to the load. The corresponding switching configuration is illustrated in Figure 11.

Table 2 shows that with changes in wind speed, the DC generator produces a higher output voltage as well as the battery voltage, the output voltage of the inverter and transformer increases.

Figure 12 illustrates the inverter output voltage waveform after being amplified using a transformer to 270 Vpp before filtering. The horizontal axis indicates time (t), whereas the vertical axis represents the measured voltage magnitude (V).

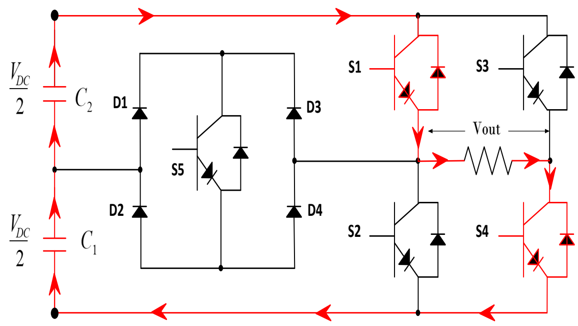

Figure 9 The current flow at the Vdc level.

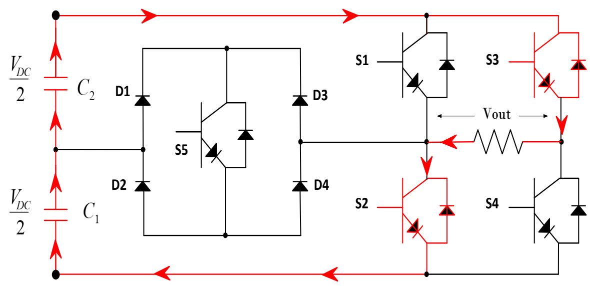

Figure 10. The direction of current flow at the –Vdc level.

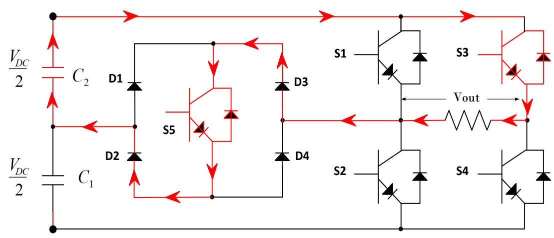

Figure 11. The current flow at the –Vdc/2 level.

Table 2.
Test simulation results.

Wind Speed (m/s)	GDC Voltage (V)	Battery (V)	Inverter Output	Trafo (V)	THD (%)
20	71/1.62	14.47	14.6/0.145	260	28.48
25	113.4/3.13	14.64	14.65/0.147	260.15	28.48
30	207.4/6.14	14.97	15/0.15	270.5	28.48
35	329/10.27	15.27	15.2/0.17	272	28.48

Table 3.
Status of the switch when operating at each level.

Voltage Level	S_1	S_2	S_3	S_4	S_5
0	OFF	ON	OFF	ON	OFF
Vdc/2	OFF	OFF	OFF	ON	ON
Vdc	ON	OFF	OFF	ON	OFF
Vdc/2	OFF	OFF	ON	OFF	ON
Vdc	OFF	ON	ON	OFF	OFF

In Figure 13, the THD index is 28.48 % before filtering and is constant even though there are changes in wind speed. This shows that the increase in output voltage is not accompanied by changes in the current and voltage waveforms. However, the THD value is still high, so a filter or number of levels needs to be increased to a greater level. Table 3 explains the state of each switch when operating at each level.

C. LCL filter analysis

From the system design, the parameter values are known as $L_1 = L_2 = 0.01$ H, thus $L_1 + L_2 = 0.02$ H, $L_1.L_2 = 0.0001H^2, C = 1$ mF $= 0.001$F . Using (6), the resonance frequency can be calculated as $f_r = 71$Hz. Analysis is done with respect to $f_s = 200$ Hz. In an ideal LCL filter design, the following condition must be satisfied, $f_{fundamental} < f_r < \frac{f_s}{2}$ $f_{fundamental} = 50\ Hz$ and $\frac{f_s}{2} = \frac{200}{100} = 100$ Hz, then the resonance frequency lies within the safe region relative to the switching frequency. The LCL filter provides an attenuation slope of −60 dB/decade, making it more effective in suppressing high-frequency harmonics than a conventional LC filter (−40 dB/decade). With a switching frequency of 200 Hz, dominant harmonics occur at 200 Hz, 400 Hz, and 600 Hz. Since the resonance frequency is 71 Hz, components above this frequency are attenuated, significantly suppressing the 200 Hz switching harmonics. Consequently, the filter effectively reduces THD and smooths stepped inverter waveforms into signals closer to a sinusoidal form.

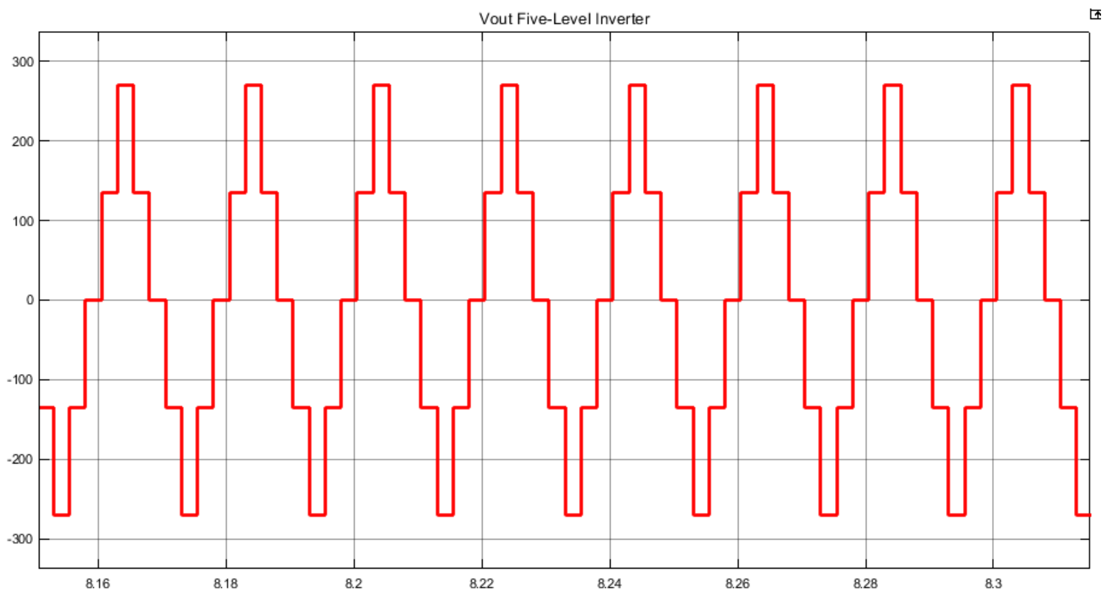

Figure 12. Form of five-level inverter waveform before filtering.

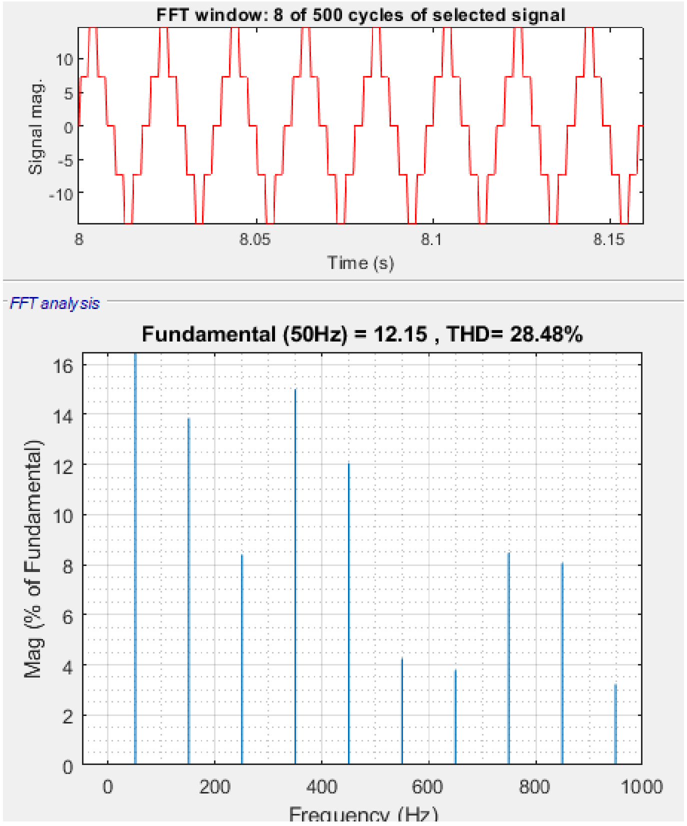

Figure 13. THD index of five levels.

Figure 14 shows the output voltage waveform after filtering under steady-state conditions. The waveform appears stable and nearly sinusoidal with consistent amplitude and frequency, indicating effective suppression of transient components. Although slight ripple remains at the peaks and valleys due to residual harmonics, its magnitude is relatively small compared to the first-order component. The obtained results confirm the proper performance of the filter in improving power quality, making the output voltage suitable for supplying electrical loads, particularly those sensitive to harmonic distortion.

D. Total harmonic distortion analysis

Total Harmonic Distortion (THD) was analyzed under R, RL, and RC load conditions to evaluate the capability of the filter to improve output waveform quality by minimizing harmonic distortion components. The THD values for each load condition are compared and expressed in percentage (%) to indicate the level of harmonic attenuation achieved.

The FFT spectrum of the system output voltage with a resistive load is presented in Figure 15, showing steady-state operation with a stable periodic waveform. The spectrum indicates a 50 Hz fundamental

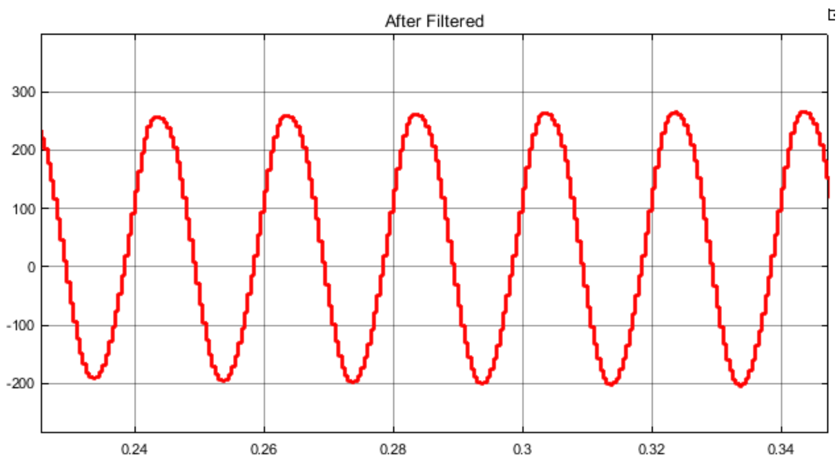

Figure 14. The transformer output voltage after filtering.

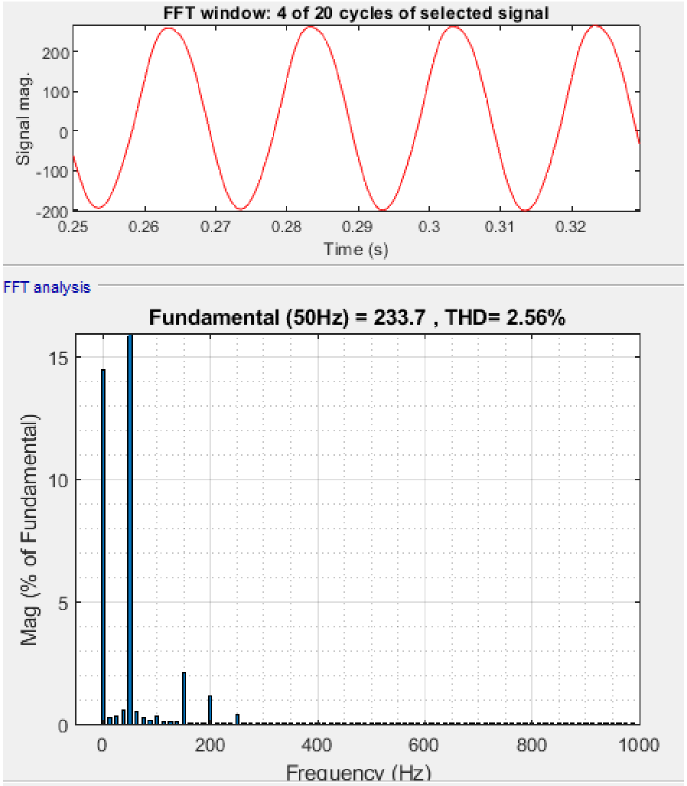

Figure 15. Resistive Load THD.

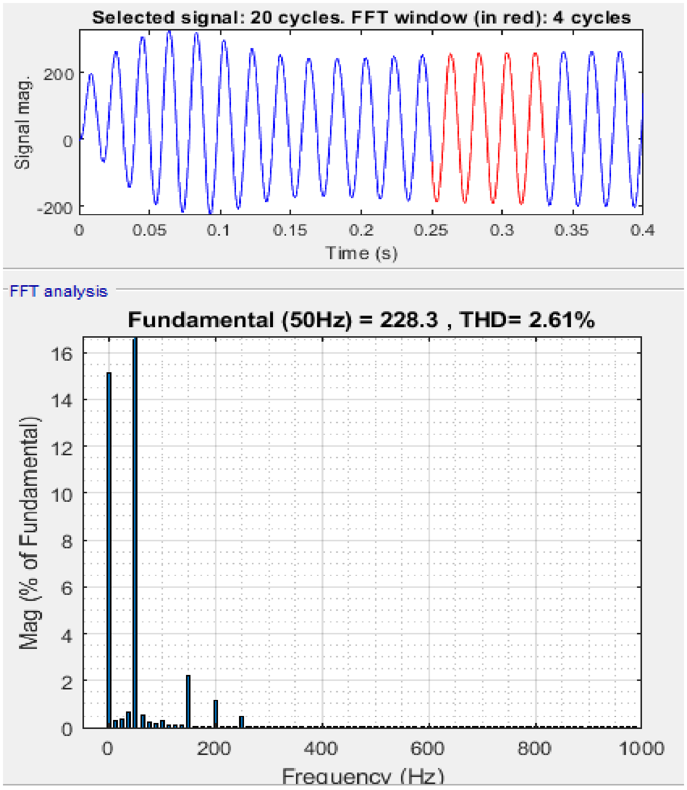

Figure 16. Resistive-Inductive (RL Load).

component with an amplitude of 233.7 and a THD of 2.56 %, demonstrating low harmonic distortion. These results confirm that the five-level inverter with an LCL filter provides good output voltage quality under resistive load conditions.

The output voltage frequency spectrum analyzed using FFT is shown in Figure 16 under steady-state conditions. The waveform is stable and periodic, indicating steady-state operation. The spectrum shows a 50 Hz fundamental component with a magnitude of

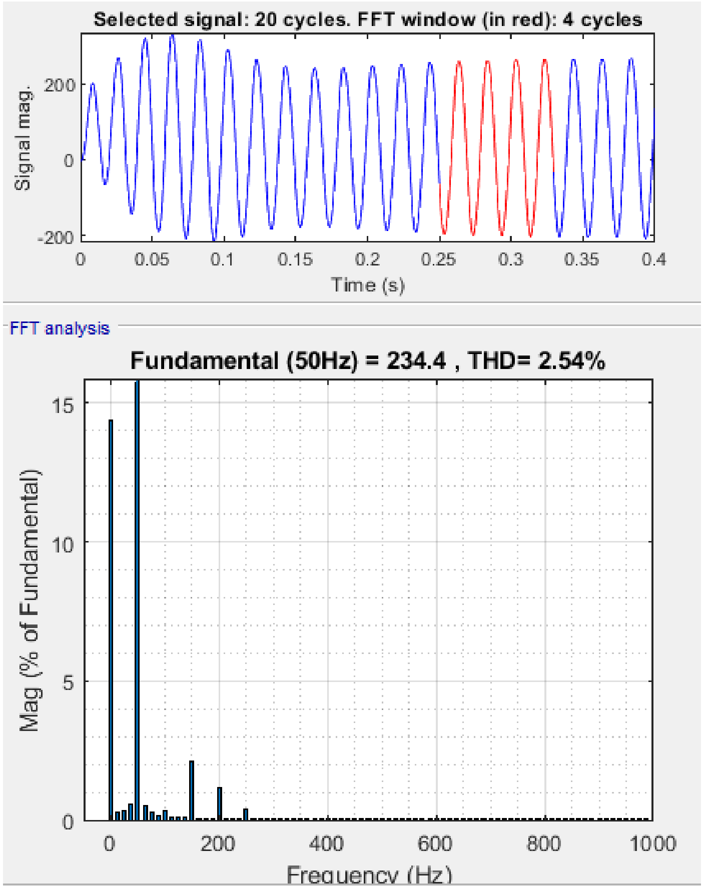

Figure 17. Resistive–Capacitive load THD.

228.3 and a THD of 2.61 %, demonstrating that the five-level inverter with an LCL filter effectively suppresses harmonics and produces high-quality output voltage.

Figure 17 shows the Fast Fourier Transform (FFT) spectrum of the output voltage under steady-state conditions with an RC load. The spectrum shows a 50 Hz fundamental component with a magnitude of 234.4 and a THD of 2.54 %, indicating low harmonic distortion. This confirms that the five-level inverter with an LCL filter provides good output voltage quality under RC load.

IV. Conclusion

This research has successfully developed and modeled a wind energy–based power generation system integrating a DC generator, an asynchronous buck converter, a five-level inverter with a reduced number of switches, an LCL filter, and a step-up transformer using MATLAB/Simulink. The proposed inverter topology utilizes only five switches, reducing component count, switching losses, and system complexity compared to conventional cascaded H-bridge multilevel inverters. Simulation results show that the five-level inverter produces a stepped AC output voltage with an amplitude of approximately 270 V at 50 Hz. However, before filtering, the output voltage exhibits a relatively high THD value of 28.48 %. The implementation of an LCL filter ($L_1 = L_2 = 0.01$ H and C = 1 mF) significantly improves power quality by reducing harmonic distortion. The THD values after filtering are 2.56 % for resistive loads, 2.61 % for resistive–inductive (RL) loads, and 2.54 % for resistive–capacitive (RC) loads. These results comply with the IEEE 519 standard requirement of THD below 5 %. The analysis confirms that the LCL filter demonstrates effective performance in eliminating high-frequency harmonic components generated by the inverter switching operation, producing a near-sinusoidal output waveform under various load conditions. Additionally, the integration of a transformer enables voltage step-up without increasing the DC-link voltage, improving system flexibility and safety through galvanic isolation. Overall, the proposed system demonstrates good performance, low harmonic distortion, and adaptability under different load variations, making it suitable for small-scale wind power plant applications and renewable energy–based distributed generation systems.

Acknowledgements

We would like to thank Gunadarma University as the author's institution for its support and assistance during the research. Similarly, thanks to the advice from Prof. Yanusyah Haroen, as technical advisor, in preparing this research report.

Declarations

Author contribution

Setiyono, B. Dwinanto, and D. Nur'ainingsih contributed equally as the main contributor of this paper. All authors read and approved the final paper.

Funding statement

This research did not receive any specific grant from funding agencies in the public, commercial, or not-for-profit sectors.

Competing interest

The authors declare that they have no known competing financial interests or personal relationships that could have appeared to influence the work reported in this paper.

The use of AI or AI-assisted technologies

During the preparation of this work, the authors used ChatGPT (OpenAI) in order to assist with drafting, language editing, grammar correction, and improving the clarity and readability of the manuscript. After using this tool, the authors reviewed, verified, and edited the content as needed and take full responsibility for the content of the publication.

Additional information

Reprints and permission: information is available at https://mev.brin.go.id/.

Publisher's Note: National Research and Innovation Agency (BRIN) remains neutral with regard to jurisdictional claims in published maps and institutional affiliations.

References

[1] N. A. Pambudi et al., "The future of wind power plants in Indonesia: Potential, challenges, and policies," *Sustainability*, vol. 17, no. 3, Art. no. 1312, 2025.

[2] B. P. Resosudarmo, J. F. Rezki, and Y. Effendi, "Prospects of energy transition in Indonesia," *Bull. Indones. Econ. Stud.*, vol. 59, no. 2, pp. 149–177, 2023.

[3] F. Portillo, A. Alcayde, R. M. Garcia, M. Fernandez-Ros, J. A. Gazquez, and N. Novas, "Life cycle assessment in renewable energy: Solar and wind perspectives," *Environments*, vol. 11, no. 7, Art. no. 147, 2024.

[4] T. Hidayat, "Wind power in Indonesia: Potential, challenges, and current technology overview," in Indonesia Post-Pandemic Outlook: Strategy Towards Net-Zero Emissions by 2060 from the Renewables and Carbon-Neutral Energy Perspectives, pp. 109–132, 2022.

[5] D. L. Pristiandaru and N. A. Pambudi, "Wind energy in Indonesia: Current status, potential, challenges, opportunities, and future policy," *Indones. J. Energy*, vol. 2, no. 2, pp. 65–73, 2019.

[6] M. A. M. Kamal, A. Bostani, J. L. Webber, A. Mehbodniya, and R. Mishra, "Total harmonic distortion reduction-based energy harvesting using a grid-based three-phase system and integral-derivative control," *Comput. Electr. Eng.*, vol. 109, pp. 1–13, 2023.

[7] Y. Hoon, M. A. Mohd Radzi, M. K. Hassan, and N. F. Mailah, "Control algorithms of shunt active power filter for harmonics mitigation: A review," *Energies*, vol. 10, no. 12, Art. no. 2038, 2017.

[8] M. Benaouadj, Z. Boumous, and S. Boumous, "Active harmonic filtering for improving power quality of an electrical network," *J. Eur. Syst. Autom.*, vol. 55, no. 3, pp. 397–403, 2022.

[9] M. S. Sujatha, S. Sreelakshmi, E. Parimalasundar, and K. Suresh, "Mitigation of harmonics for five-level multilevel inverter with fuzzy logic controller," *Electr. Eng. Electromech.*, no. 4, pp. 52–56, 2023.

[10] M. Sarebanzadeh, M. A. Hosseinzadeh, C. Garcia, E. Babaei, S. Islam, and J. Rodriguez, "Reduced-switch multilevel inverter topologies for renewable energy sources," *IEEE Access*, vol. 9, pp. 120580–120595, 2021.

[11] Marhatang *et al.*, "Design of wind power generator for tambak houses," *J. Electr. Technol. UMY*, vol. 7, no. 1, pp. 20–28, 2023.

[12] W. Yandi, M. Y. Puriza, M. Jumnahdi, and R. Kurniawan, "Comparative efficiency of solar panels and wind turbine DC generators as green energy sources in Bangka Island," *IOP Conf. Ser.: Earth Environ. Sci.*, vol. 599, Art. no. 012037, 2020.

[13] M. S. Sakib, D. T. Griffith, S. Hossain, S. Bayat, and J. T. Allison, "Intracycle RPM control for vertical-axis wind turbines," *Wind Energy*, vol. 27, no. 3, pp. 202–224, 2024.

[14] S. U. Handayani, "Effect of winglets on improving wind turbine performance," *J. Vocat. Stud. Appl. Res.*, vol. 3, no. 1, pp. 5–8, 2021.

[15] F. Merahi et al., "Power control of an autonomous wind energy conversion system based on a permanent magnet synchronous generator with integrated pumping storage," *Sci. Rep.*, vol. 14, Art. no. 29776, 2024.

[16] D. Devin et al., "Design and CFD simulation of guide vane for multistage Savonius wind turbine," *J. Mechatron. Electr. Power Veh. Technol.*, vol. 14, no. 2, pp. 186–197, 2023.

[17] P. Kinsler, "Faraday's law and magnetic induction: Cause and effect, experiment and theory," *Physics*, vol. 2, no. 2, pp. 150–163, 2020.

[18] Z. Yang, X. Sun, R. Han, R. Shang, Z. Chen, and X. Liu, "Influence of winding configurations and stator/rotor pole combinations on field back-EMF ripple in

switched-flux hybrid-excited machines," *Energies*, vol. 17, no. 23, Art. no. 5906, 2024.
[19] A. Sujono, F. Adriyanto, H. Maghfiroh, J. S. Saputro, and A. Ramelan, "Variable-speed DC generator voltage control using a multistage comparator," *J. Electr. Electron. Inf. Commun. Technol.*, vol. 3, no. 1, pp. 18–22, 2021.
[20] Mudakir, Aripriharta, and A. P. Wibawa, "Analysis of battery energy storage system performance in reducing the impact of variable renewable energy generation intermittency on the electricity system," *J. Mechatron. Electr. Power Veh. Technol.*, vol. 15, no. 2, pp. 158–176, 2024.
[21] I. Sarbu and C. Sebarchievici, "A comprehensive review of thermal energy storage," *Sustainability*, vol. 10, no. 1, Art. no. 191, 2018.
[22] M. Danko, J. Adamec, M. Taraba, and P. Drgona, "Overview of battery state-of-charge estimation methods," *Transp. Res. Procedia*, vol. 40, pp. 186–192, 2019.
[23] W. Guan and X. Huang, "A modular active balancing circuit for redox flow battery applied in energy storage system," *IEEE Access*, vol. 9, pp. 127548–127558, 2021.
[24] N. H. Baharudin, T. M. N. T. Mansur, F. A. Hamid, R. Ali, and M. I. Misrun, "Performance analysis of DC–DC buck converter for renewable energy application," *J. Phys.: Conf. Ser.*, vol. 1019, Art. no. 012020, 2018.
[25] W. Indrasari *et al.*, "Development of DC–DC buck converter for solar panel energy storage through load optimization and feedback circuit," *Spektra: J. Fis. dan Apl.*, vol. 8, no. 3, pp. 143–152, 2023.
[26] D. Khan, M. Qais, I. Sami, P. Hu, K. Zhu, and A. Y. Abdelaziz, "Optimal LCL-filter design for a single-phase grid-connected inverter using metaheuristic algorithms," *Comput. Electr. Eng.*, vol. 110, Art. no. 108857, 2023.
[27] H. Adamas-Pérez, M. Ponce-Silva, J. D. Mina-Antonio, A. Claudio-Sánchez, O. Rodríguez-Benítez, and O. M. Rodríguez-Benítez, "A new LCL filter design method for single-phase photovoltaic systems connected to the grid via micro-inverters," *Technologies*, vol. 12, no. 6, Art. no. 89, 2024.
[28] R. Eswaramoorthi, "Development of a low-harmonic-distortion three-phase inverter for renewable grid integration," *Trans. Power Electron. Renew. Energy Syst.*, vol. 2, no. 2, pp. 20–28, 2026.
[29] G. Priyanka, J. S. Kumari, D. Lenine, P. S. Varma, S. S. Madhuri, and V. Chandu, "MATLAB/Simulink-environment-based power quality improvement in photovoltaic system using multilevel inverter," *Electr. Eng. Electromech.*, vol. 45, no. 2, pp. 43–48, 2023.
[30] Suroso, D. T. Nugroho, A. N. Azis, and T. Noguchi, "Simplified five-level voltage-source inverter with level-phase-shifted-carrier-based modulation technique," *Indones. J. Electr. Eng. Comput. Sci.*, vol. 13, no. 2, pp. 461–468, 2019.
[31] M. Karakılıç, H. Hataş, and M. N. Almali, "Design of a 21-level multilevel inverter with a minimum number of devices," *Int. J. Circuit Theory Appl.*, vol. 51, no. 12, pp. 5705–5723, 2023.
[32] E. Parimalasundar, S. Muthukaruppasamy, R. Dharmaprakash, and K. Suresh, "Performance investigations of a five-level reduced-switch-count H-bridge multilevel inverter," *Electr. Eng. Electromech.*, vol. 6, no. 6, pp. 58–62, 2023.
[33] M. I. D. Prasetyo *et al.*, "Integration of a bidirectional cell in a quasi-Z-source inverter for CMV reduction and pure sinusoidal waveform," *J. Mechatron. Electr. Power Veh. Technol.*, vol. 16, no. 2, pp. 266–277, 2025.